

AD-A190 490

Approved for Release by NSA on 05-08-2014 pursuant to E.O. 13526

Douglas Aircraft Company

MCDONNELL DOUGLAS

OSCILLATING AIRFOILS - ACHIEVEMENTS AND CONJECTURES

by

Tuncer Cebeci



September 1987

Accession For	
NTIS CRA&I	<input checked="" type="checkbox"/>
DTIC TAB	<input type="checkbox"/>
Unannounced	<input type="checkbox"/>
Justification	
By	
Distribution	
Availability Codes	
Dist	Availability Codes
A-1	

This research was supported under
The Air Force Office of Scientific Research
Contract F49620-87-C-0004.

Copy number

Report number

MDC K0535

OSCILLATING AIRFOILS -
ACHIEVEMENTS AND CONJECTURES

Technical

Revision date

Revision letter

Issue date September 1987

Contract number F49620-87-C-0004

Prepared by : Tuncer Cebeci
Staff Director, Research & Technology

Approved by:



Tuncer Cebeci
Staff Director,
Research & Technology
Aircraft Configuration
and Performance Subdivision



J. T. Callaghan
Acting Manager,
Aircraft Configuration
and Performance Subdivision



M. Klotzsche
Program Manager, CRAD and
Cooperative Technology Development

DOUGLAS AIRCRAFT COMPANY

MCDONNELL DOUGLAS



ABSTRACT

Recent developments and applications of an interactive boundary-layer procedure for unsteady flows are reviewed. The emphasis is on a model problem corresponding to an oscillating thin airfoil in laminar flows and results are reported for different amplitudes and frequencies of oscillation. The use of the characteristic box scheme, with its stability criterion, are shown to allow the accurate calculation of reverse flows and the interaction procedure removes the singularity to allow calculation through regions of separated flow. Although the current focus of the interactive boundary-layer procedure has been on the leading-edge region, it has general applicability and, together with models for transition and turbulent flows, it can provide the basis for a method to deal with oscillating airfoils and wings and the rapid movement of fixed-wing arrangements at angles of attack up to and beyond those of dynamic stall.

Calculations at high angles of attack indicate that the behavior of the unsteady separated leading-edge flow has similarities to steady flows downstream of surface corrugations. The use of linear stability theory in the latter case shows that the location of the onset of transition moves upstream with severity of corrugation and can move inside the separation bubble. In practice this means that the bubbles will be shortened and analogy with unsteady flows suggests that transition may play an important role and preclude the existence of the long separation bubbles determined by the laminar-flow calculations.

TABLE OF CONTENTS

	<u>Page</u>
1.0 Introduction	1
2.0 Model Problem	4
3.0 Achievements	6
3.1 Moving Stagnation-Point Problem	6
3.2 Large Flow Reversals and the Need for Numerical Accuracy	7
3.3 Effects of Unsteadiness and Interaction on Separated Flows	11
4.0 Conjectures; Separation Bubbles and Transition	15
5.0 Concluding Remarks	19
6.0 References	21

LIST OF FIGURES

<u>No.</u>	<u>Title</u>	<u>Page</u>
1	Variation of the velocity profiles for $\omega = \pi/30$ near the stagnation region for different values of ωt , (a) 90, (b) 180, (c) 270, (d) 360	6
2	Variation of the velocity profiles for $\omega = \pi/3$ near the stagnation region for different values of ωt , (a) 90, (b) 180, (c) 270, (d) 360. The dashed line indicates the locus of zero u-velocity . . .	7
3	Variation of: displacement thickness, $\tilde{\delta}^*$ with ξ for the oscillating airfoil, $A = 1$, $\omega = 0.1$, obtained with the zig-zag scheme. . . .	8
4	Effect of the coarse and fine meshes on the variation of the stability parameter β with ωt	9
5	Effect of the coarse and fine meshes on the variation of the (a) stability parameter β , and (b) wall shear f_w'' with ξ	10
6	Results obtained with the characteristic_box scheme for $\omega = 0.1$. Variation of (a) displacement thickness $\tilde{\delta}^*$ and (b) wall shear f_w'' with ξ	10
7	Variation of wall shear f_w'' with ξ for (a) $\omega = 0.01$, (b) $\omega = 0.001$	11
8	Effect of interaction on the variation of wall shear f_w'' with ξ for (a) $\omega = 0.01$, (b) $\omega = 0.001$. $R = 10^4$	12
9	Effect of interaction on the variation of wall shear parameter f_w'' for a steady flow at $R = 10^4$	14
10	Separation bubbles and their breakdown - explanation from steady flow (i.e. $\omega = 0$), $R = 10^5$	16
11	Accuracy of stability approach to transition. Steady flow over bumps, data of Fage [34]	17

1.0 INTRODUCTION

The experimental investigations of McCroskey, McAlister and Carr [1], Carr, McAlister and McCroskey [2], Dadone [3], Francis, Keese and Rettle [4], Daley and Jumper [5], Francis and Keese [6], Lorber and Covert [7] and Lorber and Carta [8] were prompted by the need to provide better understanding of the flow characteristics of oscillating airfoils. It is important, for example, that the rotor blades of helicopters do not experience dynamic stall and the experiments have demonstrated that stall is preceded by a near-surface vortex associated with separation of the unsteady boundary layer. It is likely that the vortex stems from a laminar separation bubble which, with increasing angle of attack, grows until it becomes unstable and bursts to form a vortex which rolls and grows. These experiments have been complemented by a number of computational investigations which involve the solution of the Navier-Stokes equations [9], and of the boundary-layer equations sometimes coupled to inviscid flow equations as, for example, by Cebeci and Carr [10-12]. As yet, the calculation methods have not been successful in representing the measurements and a procedure to provide accurate representation of oscillating airfoil flows for a wide range of flow conditions including dynamic stall remains to be developed. A useful review covering all aspects of the subject has been provided by Lang [13] and important applications considered by Herbst [14].

The calculation of flow over an oscillating airfoil by an interactive boundary-layer scheme makes use of inviscid and viscous flow methods and couples them by a special procedure. The success and accuracy of this method depends on the accuracy of each component including the procedure used to link the inviscid and viscous flow methods. In general the inviscid flow methods are based on panel methods, such as those of Geissler [15], Maskew and Dvorak [16] and Teng [17], and their accuracy and ability to solve flow problems of great complexity are well known. The viscous-flow methods, on the other hand, are not so well developed and their application to time-dependent flows has not received the same interest as to steady flows. The calculation of unsteady flows with large regions of flow reversal has been confined mostly to model problems involving flows such as the laminar flow over a circular cylinder impulsively started from rest. The emphasis has been on the solution of the boundary-layer equations for a prescribed pressure distribution and exploration of the relationship between flow singularity and separation. In spite of

the apparent simplicity of this model problem, many difficulties were encountered and some remain to be solved.

The calculation of boundary layers on an oscillating airfoil poses some problems that are different than those considered in other unsteady boundary-layer flows. Perhaps the most important of these is the calculation of the upstream boundary conditions in the (t,y) plane at some $x = x_0$ which are needed in the solution procedure. Contrary to steady flows where the streamwise velocity u is identically zero across the shear layer at the stagnation point, this is not the case in time-dependent flows; flow reversals occur due to the movement of the stagnation point and cause the locus of zero u -velocity to vary with space requiring the use of a special numerical method. It should be emphasized that the problem of the upstream boundary conditions has a physical counterpart and is not solely numerical. The evolution of an unsteady flow at high angles of attack can involve the formation of a vortex in the region close to the leading edge and is associated with the onset of dynamic stall. Thus it is imperative that calculations of the flow in the upstream region be accurate.

The difficulties in the solution of the time-dependent boundary-layer equations depend on whether or not there is flow reversal across the boundary layer. In its absence, there are several numerical methods that can be used to solve the equations including those of Crank-Nicholson [18] and Keller [19]. In the presence of flow reversal, however, it is necessary to use a scheme like the characteristic box method which is based on the solution of time-dependent boundary-layer equations along the local streamlines as described by Keller [20] and Cebeci [21].

This scheme allows the step sizes in the time and streamwise directions to be automatically adjusted to ensure that the region of backflow, as determined by the local streamlines, does not violate a stability condition like that of Courant, Friedrichs and Lewy (CFL). Although the zig-zag scheme of Krause et al. [22] can also be used for this purpose, it can be inaccurate in regions of large flow reversal since the orientation of numerical mesh is chosen a priori, as discussed by Cebeci [21] and Cebeci, Khattab and Schimke [23].

The coupling between inviscid and viscous flow methods has attracted even less attention than the above and most work has again been directed to the development of methods for steady flows. Two coupling procedures have been proposed and that suggested by Veldman [24] offers greater flexibility than that of LeBalleur [25] and Carter [26] and has been developed for two-dimensional airfoils by Cebeci and his associates [27]. It has also been extended to three-dimensional flows, albeit with strip theory and quasi-three-dimensional approximations, including flow over swept wings [28], and leading-edge separation bubbles on thin wings [29].

The flow singularity in steady flows corresponds to the vanishing of the wall shear and the boundary-layer equations can be solved routinely with a prescribed pressure distribution up to this point; there are no questions regarding the accuracy of the solutions. The u -velocity does not exhibit flow reversals across the layer and the inaccuracies resulting from the rapid variation of flow conditions near the separation location can be accounted for by taking small steps in the streamwise direction. It is also known that with interaction, that is computing the external velocity as part of the solution, this singularity can be removed and separated flows can be calculated for both laminar and turbulent flows. Time-dependent flows follow a similar pattern and concentration on the "proper" definition of flow singularity or separation, ensures that any singularity can be removed by interaction. This requires that the singularity is identified and that the region of reverse flow, which usually precedes the singularity at separation of an unsteady flow, be calculated accurately. Inaccuracy in the calculation of the reverse flows can lead to breakdown of the solution procedure and the erroneous assumption that it is caused by a singularity. An interactive boundary-layer method may not remedy this situation since its success depends on the accuracy of the solutions of the boundary-layer equations. We shall discuss this point further in this report.

2.0 MODEL PROBLEM

This report reviews some of the results which have been obtained with a numerical procedure designed to overcome the problems outlined above. Thus, with support from the Air Force Office of Scientific Research, AFOSR, we have addressed fundamental aspects of the problem including the determination of upstream boundary conditions, the relationship between singularity and separation, and the development of an interactive procedure. To overcome the corresponding difficulties, we have developed a novel method to deal with the leading-edge region (Section 3.1), an accurate numerical method for the region of reverse flow (Section 3.2) and an interactive procedure which, together with a numerical stability requirement, have allowed us to study the nature of the singularity and to provide fundamental understanding of the mechanisms of the region of recirculating flow near to the leading edge of an oscillating airfoil (Section 3.3). We have also made use of the linear stability theory and analogy between unsteady flow at high angle of attack and steady flow over a surface with corrugation to conjecture that long separation bubbles obtained for laminar flows may not exist in practice. It appears likely that transition will occur within these bubbles with consequent reduction in their length. This is discussed in Section 4.

To accomplish these objectives, we have considered the model problem of laminar flow over a thin airfoil with a thickness ratio of γ ($\equiv b/a$) at a reduced angle of attack ξ_0 . The external velocity for a steady flow in this case can be deduced from inviscid flow to be

$$\bar{u}_e(\xi) = \frac{u_e}{u_\infty(1 + \gamma)} = \frac{\xi + \xi_0}{\sqrt{1 + \xi^2}} \quad (1)$$

where the parameter ξ is related to the surface distance s by

$$s = a\gamma^2 \int_{\xi_0}^{\xi} (1 + \xi^2)^{1/2} d\xi \quad (2)$$

Equation (2) is extended to unsteady flows by introducing time dependence in the form

$$\bar{u}_e(\xi, t) = \frac{\xi + \xi_{\text{eff}}}{\sqrt{1 + \xi^2}} \quad (3)$$

where

$$\xi_{\text{eff}} = \xi_0 (1 + A \sin \omega t)$$

The resulting flow contains the essential ingredients of the leading-edge region of an oscillating airfoil including the moving stagnation point with consequent reverse flows, the possibility of boundary-layer separation and reattachment and their dependence upon the amplitude of oscillation, A , the frequency ω and distance from the leading edge, s . It also permits comparison with the equivalent steady flows for which calculations have been reported by, for example, Cebeci, Stewartson and Williams [30].

The coupling between the inviscid and viscous flows is accomplished by writing the edge boundary condition in the boundary-layer equations as the sum of the inviscid velocity $u_e^0(\xi, t)$ and a perturbation velocity $\delta u_e(\xi, t)$, that is,

$$\text{at } y = \delta \quad u_e(\xi, t) = u_e^0(\xi, t) + \delta u_e(\xi, t) \quad (4)$$

and $\delta u_e(\xi, t)$ is obtained from the Hilbert integral given by

$$\delta u_e(\xi, t) = \frac{1}{\pi} \int_{s_a}^{s_b} \frac{d}{ds} (u_e \delta^*) \frac{d\sigma}{s - \sigma} \quad (5)$$

with the interaction region confined between s_a and s_b and with $u_e^0(\xi, t)$ given by Eq. (3). Further details can be found in Ref. 30.

The emphasis of the present work has been on the leading-edge region and makes use of an expression for the freestream boundary condition which has been obtained by solution of the inviscid-flow equations. The interactive boundary-layer method is, however, general so that it can involve any solutions to inviscid-flow equations and an entire airfoil with laminar, transitional and turbulent flow.

3.0 ACHIEVEMENTS

The following three subsections highlight results obtained, respectively, with the special procedure to deal with the stagnation point, to show the importance of numerical accuracy in regions of reverse flow and to report and discuss the effects of unsteadiness on recirculation bubbles.

3.1 Moving Stagnation-Point Problem

The numerical difficulties associated with the moving stagnation point exist in a number of flows including those associated with turbomachinery, as discussed by Cebeci, Simoneau and Platzer [31]. Thus the wakes generated by moving rotor blades lead to movement of the stagnation points on the downstream of stator blades. An accurate numerical scheme has been developed to solve this problem and, as described by Cebeci et al. [31], makes use of the characteristic box scheme in an iterative manner to deal with the flow reversals.

Figures 1 and 2 show calculated results for the model problem with two circular frequencies, $\omega = \pi/30$, $\pi/3$, and $\xi_0 = 1$, $A = -0.5$. They allow examination of the effect of frequency on the calculated velocity profiles in the vicinity of the stagnation point. Figure 1 shows that the locus of the u -velocity on time lines $t = \pi/2$ and π is essentially the same as in the steady case and as a result there are no flow reversals in the velocity profiles. However, as can be seen from Figure 2, flow reversals begin to occur around the stagnation point with increase in the frequency to $\pi/3$ and become more prolonged as time

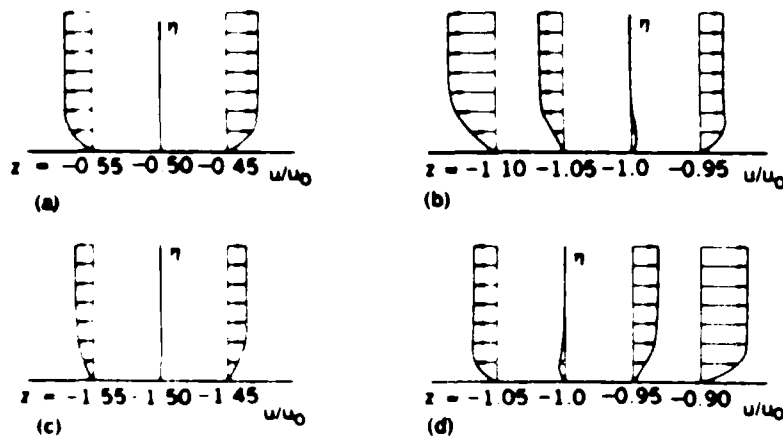


Fig. 1. Variation of the velocity profiles for $\omega = \pi/30$ near the stagnation region for different values of ωt , (a) 90, (b) 180, (c) 270, (d) 360.

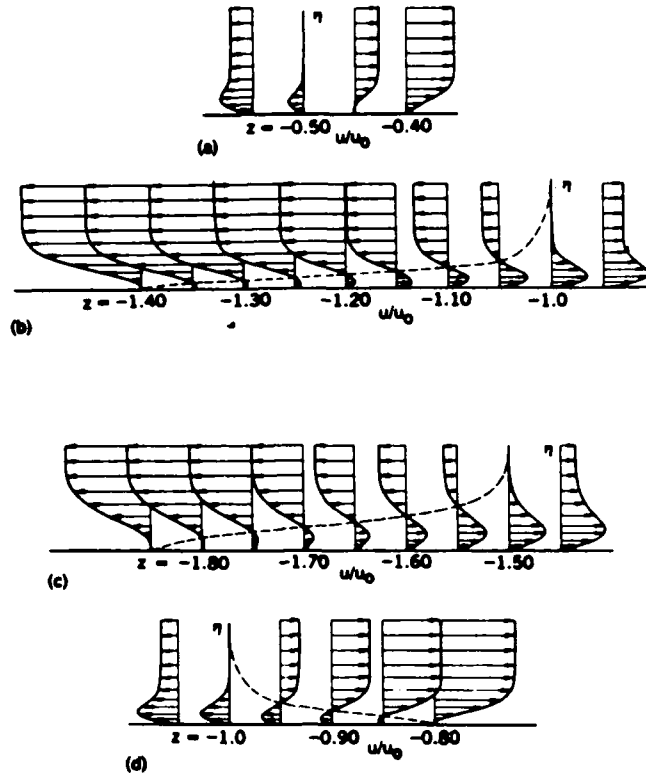


Fig. 2. Variation of the velocity profiles for $\omega = \pi/3$ near the stagnation region for different values of ωt , (a) 90, (b) 180, (c) 270, (d) 360. The dashed line indicates the locus of zero u -velocity.

increases to $\omega t = 3\pi/2$. At $\omega t = 2\pi$, the region of flow reversal is reduced but is not zero as it was at $\omega t = 0$.

3.2 Large Flow Reversals and the Need for Numerical Accuracy

Our calculations for the model problem were arranged to parallel those reported by Cebeci [21] for the flow over a circular cylinder. Thus the zig-zag and the characteristic box schemes were used with time and distance steps chosen arbitrarily and the calculations repeated with values in agreement with a stability criterion. The results of Fig. 3 for $\omega = 0.10$ were obtained with the zig-zag box scheme by Cebeci, Khattab and Schimke [32] for a $\Delta\xi$ -spacing specified such that $\Delta\xi_1 = 0.01$ up to $\xi = 1.7$, $\Delta\xi_1 = 0.005$ for $1.7 < \xi < 4$ and $\Delta\xi_1 = 0.01$ for $4 < \xi < 8$; the time steps Δt_n were 10 degrees for $0 < \omega t < 260^\circ$, 5 degrees for $260^\circ < \omega t < 295^\circ$, and 1.25 degrees for $295^\circ < \omega t < 360^\circ$. The calculations broke down at $\omega t = 310^\circ$, suggesting flow separation at this location.

Fig. 3 shows that the variation of the dimensionless displacement thickness $\tilde{\delta}^*$ is generally smooth except in the neighborhood of $\xi = 2.12$ and for $\omega t = 308.75^\circ$. Here R is Reynolds number based on nose radius and is defined by $(2au_\infty/\nu)$. The first sign of irregularity is the steepening of the slope of $\tilde{\delta}^*$ when $\omega t = 300^\circ$ and a local maximum of $\tilde{\delta}^*$ occurs at $\xi = 2.12$ when $\omega t = 308.75^\circ$. When the same results were plotted for a displacement velocity, $(d/d\xi)(u_e \tilde{\delta}^*)$, we observed steepening of the displacement velocity as the peak move from $\xi = 2.125$ to 2.08 with ωt changing from 300 to 308.75 degrees.

The calculations which led to Fig. 3 were repeated with the characteristic box scheme using the same coarse variations of Δt_n and $\Delta \xi_1$ and the results were identical to those obtained with the zig-zag scheme up to $\omega t = 280^\circ$. At $\omega t = 282.5^\circ$, the solutions of the zig-zag scheme were smooth and free of wiggles but those of the characteristic box scheme exhibited oscillations in f_w'' which led to their breakdown. The solutions with the zig-zag scheme, however, continued without numerical difficulties until $\omega t = 310^\circ$, where oscillations appeared and led to the breakdown of the solutions at the next time step.

The characteristic box was used subsequently with values of $\Delta \xi_1$ fixed as before and with values of Δt_n determined in accord with the stability requirement as discussed by Cebeci et al. [23]. This procedure avoided the

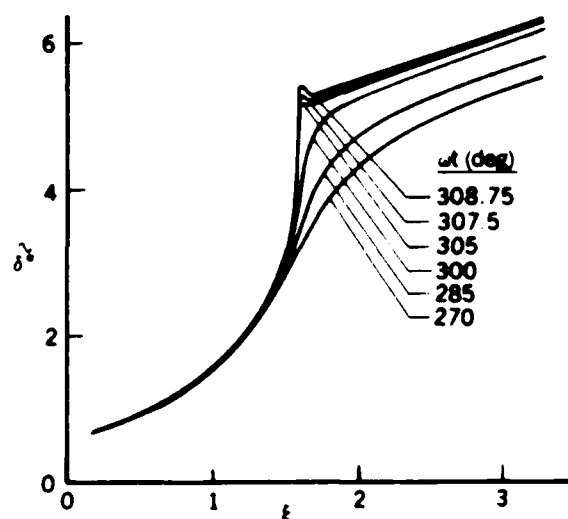


Fig. 3. Variation of: displacement thickness, $\tilde{\delta}^*$ with ξ for the oscillating airfoil, $A = 1$, $\omega = 0.1$, obtained with the zig-zag scheme.

breakdown of the solutions and, as can be seen from Fig. 4, the maximum value of the stability parameter β increases considerably with ωt so that the solutions required correspondingly smaller values of the time step. It is interesting to note that the wall-shear distributions of Fig. 5 are uninfluenced by the mesh at $\omega t = 280^\circ$ and 310° but, for $\omega t > 310^\circ$, the coarse mesh leads to large values of β and breakdown of the solutions.

Figure 6a shows the distributions of displacement thickness for values of ωt from 260° up to 360° and completes the cycle. The results up to 300° were identical with those of Fig. 3 with rapid increase of the displacement thickness corresponding to the increasing extent of flow reversal, as shown by the wall-shear distributions of Fig. 6b.

It can also be seen from this figure that the maximum displacement thickness and minimum wall shear move upstream with increasing ωt for values of ωt up to 324.5° ; this feature was also observed in the calculations performed for the circular cylinder [21]. The results obtained with the zig-zag scheme and values of Δt_n determined by the characteristic scheme for the oscillating airfoil were identical to those discussed above, and similar correspondence was obtained with the calculations performed for the circular cylinder.

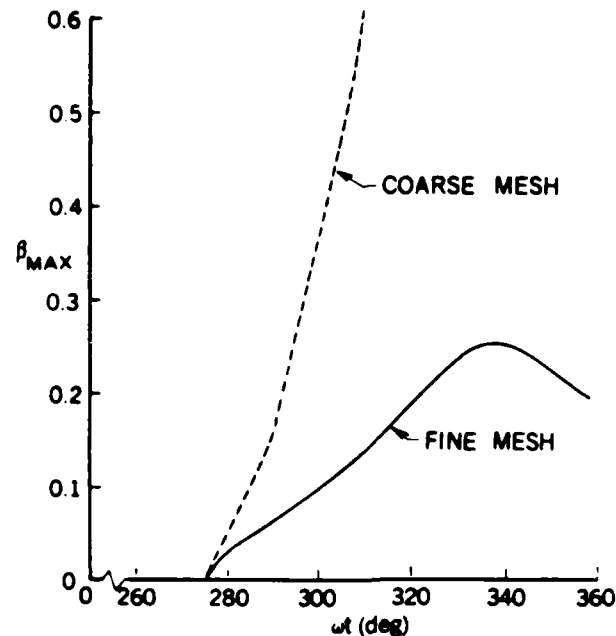


Fig. 4. Effect of the coarse and fine meshes on the variation of the stability parameter β with ωt .

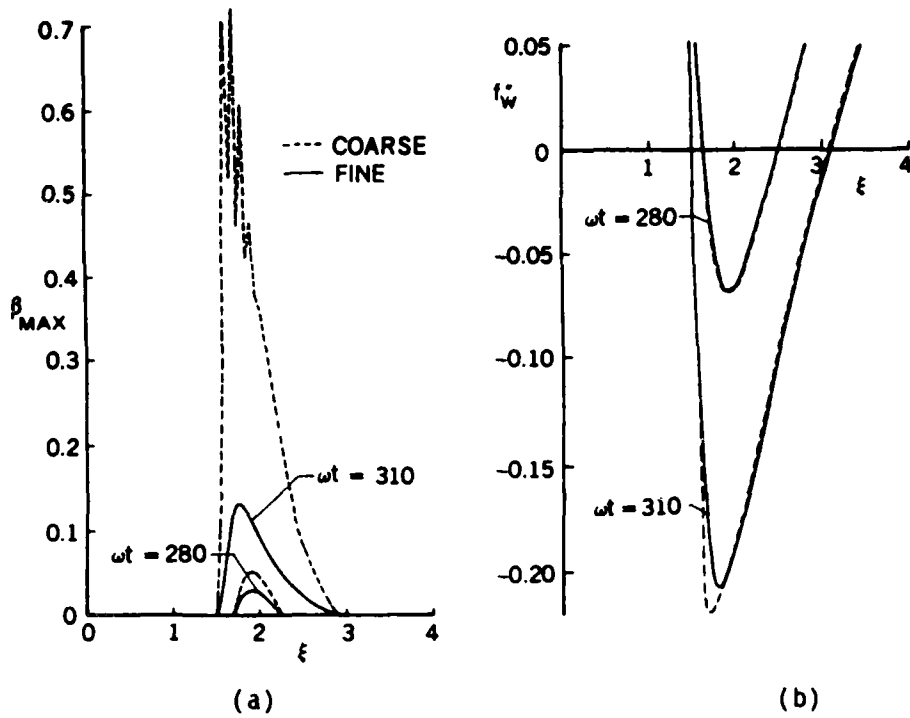


Fig. 5. Effect of the coarse and fine meshes on the variation of the (a) stability parameter β , and (b) wall shear f_w'' with ξ .

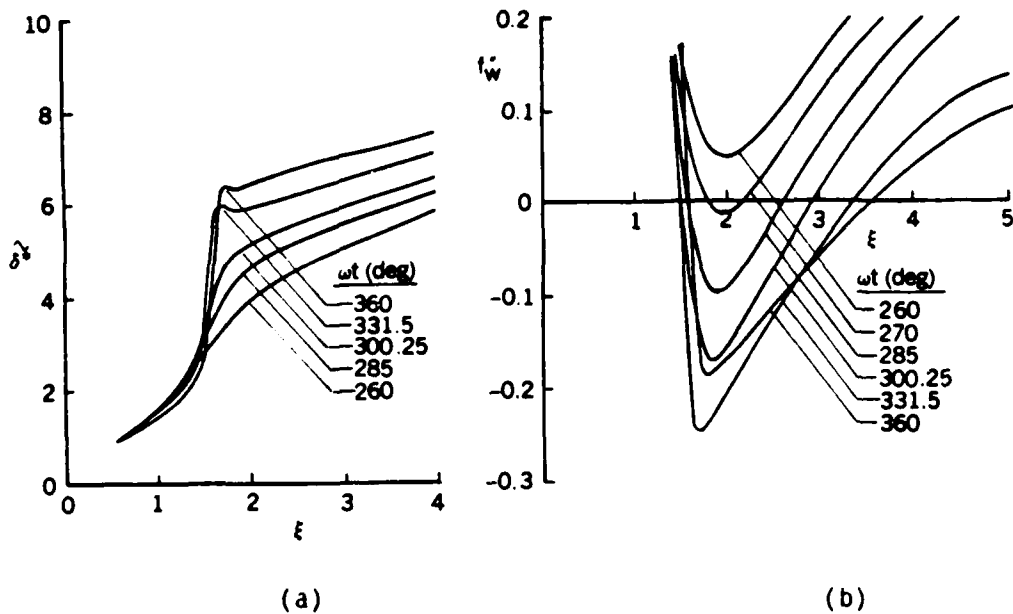


Fig. 6. Results obtained with the characteristic box scheme for $\omega = 0.1$. Variation of (a) displacement thickness δ^* and (b) wall shear f_w'' with ξ .

3.3 Effects of Unsteadiness and Interaction on Separated Flows

Figure 7 shows distributions of wall shear for frequencies $\omega = 0.01$ and 0.001 . As expected, the critical value of the reduced angle which corresponds to separation, is smaller than that for the higher frequency of Section 3.2 and closer to that of the steady state, $\xi = 1.16$. For $\omega = 0.01$, the breakdown of the solutions occurs at $\omega t = 226^\circ$, which corresponds to an effective reduced angle of $\xi_{\text{eff}} = 1.360$; for $\omega = 0.001$, the corresponding values are $\omega t = 204^\circ$ and 1.203 . We also note from Figs. 7a and 7b that the flow is a little unsteady even at these frequencies, and the solutions do not break down with the appearance of flow reversal, which increases in extent as ω changes from 0.001 and 0.01 .

The above results, and those of the previous subsection, were obtained without interaction between the solutions of inviscid-flow and boundary-layer equations. In contrast, the results of Fig. 8 were obtained with interaction and were performed in the following way. For all values of time with ωt ranging from 0° to 360° , the standard method and the leading-edge region procedure discussed in Section 3.1 were used to generate upstream boundary conditions at a short distance from the leading edge, $\xi = 0.5$. With these conditions and for each value of ωt , the inverse method was used to calculate the unsteady flow from $\xi = 0.5$ to 10 , for the specified value of Reynolds number and thickness ratio of $\gamma = 0.1$. Since the system of equations is now elliptic,

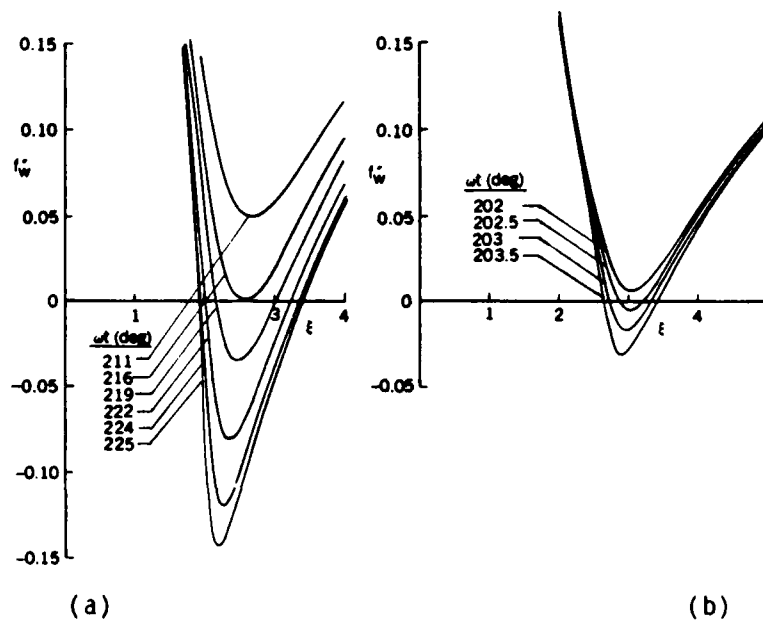


Fig. 7. Variation of wall shear f''_w with ξ for (a) $\omega = 0.01$, (b) $\omega = 0.001$.

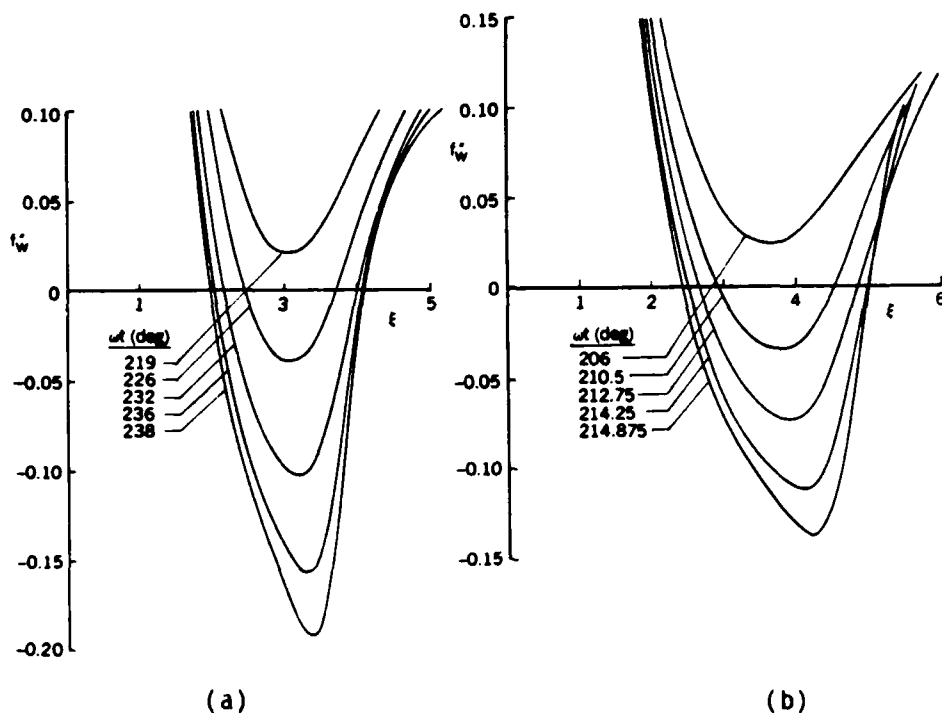


Fig. 8. Effect of interaction on the variation of wall shear f_w'' with ξ for (a) $\omega = 0.01$, (b) $\omega = 0.001$. $R = 10^4$.

sweeps in the ξ -direction were necessary to achieve a converged solution; around three sweeps were required where flow reversal was encountered and a single sweep sufficed where it did not. It is to be expected that the value of R will influence the number of sweeps and, since it is linked to physical parameters, will affect the singularity and the size of the bubble.

Figure 8 shows the results for $\omega = 0.01$ and 0.001 with $R = 10^4$. They are nearly the same as those obtained by the standard method as shown in Fig. 7 prior to flow reversal where the influence of the Reynolds number is small and increase after flow reversal. In the case of $\omega = 0.001$, for example, the standard method predicts flow reversal around $\xi_{eff} = 1.19$ (see Fig. 7) and with interaction (Fig. 8) this effective angle is between 1.219 and 1.254. The maximum negative value of the wall-shear parameter f_w'' obtained with the standard method is around -0.03 at $\xi_{eff} = 1.199$ and may be compared with the maximum value of f_w'' of -0.14 at $\xi_{eff} = 1.286$ obtained with interaction. As expected, the interaction allows the calculations to be performed at higher angles of attack than those achieved with the standard method. For $\omega = 0.001$,

the maximum α_{eff} for which calculations can be performed with the standard method is 1.199 with breakdown occurring at $\xi_{\text{eff}} = 1.209$; the corresponding values with interaction are 1.286 and 1.287. Comparison of wall-shear results with both procedures and $\omega = 0.001$ indicates that the extent of the recirculation region $\Delta\xi$ is around 0.5 for the standard case, and around 2.5 for the interactive case. The solutions do not have a singularity in the former case but do contain flow reversals and this suggests that time-dependent flows can be calculated without using an inverse procedure. As the angle of attack exceeds $\xi_{\text{eff}} = 1.199$ for $\omega = 0.001$, a singularity develops and requires an inverse procedure as in two-dimensional steady flows. This procedure allows the calculation of larger regions of reverse flow where the flow is now separated.

We see a similar picture with the greater unsteadiness corresponding to $\omega = 0.01$, for which the standard method allows calculations up to an effective angle of attack of 1.354 (Fig. 7a), a value considerably higher than 1.199 obtained at $\omega = 0.001$. The first flow reversal occurs shortly after $\xi_{\text{eff}} = 1.294$ and breakdown occurs at $\xi_{\text{eff}} = 1.360$ with maximum negative wall shear values of -0.14 at $\xi_{\text{eff}} = 1.354$ and -0.035 at $\xi_{\text{eff}} = 1.315$. The extent of the maximum reverse-flow region is now 1.5, considerably larger than for $\omega = 0.001$, and indicates that the more unsteady nature of the flow produces a bigger region of reverse flow free from singularities. For this value of ω , the interactive scheme increases the value of ξ_{eff} for which solutions can be obtained to 1.424 with breakdown occurring shortly after this value at 1.428 (see Fig. 8b). The first flow reversal occurs after $\xi_{\text{eff}} = 1.315$ with maximum negative wall shear equal to -0.19 at $\xi_{\text{eff}} = 1.424$, and the extent of the recirculation region has now increased by about 30%. Comparison of maximum wall shear values, f_w'' , at a similar value of ξ_{eff} indicates that those computed with the interactive scheme are lower than those with the standard scheme so that, for example, the interactive scheme gives $(f_w'')_{\text{max}} = -0.04$ at $\xi_{\text{eff}} = 1.36$ compared to -0.14 at $\xi_{\text{eff}} = 1.354$ with the standard method (Fig. 7a).

Since the calculations began at $\omega t = 0$ with solutions obtained by solving steady-state equations, it was necessary to confirm the extent of their influence. As a consequence, calculations were performed for a second cycle and

gave results at $\omega t = 720^\circ$ which were identical to those at $\omega t = 360^\circ$, confirming that the flow is cyclic. Examination of the results showed that the influence of the initial conditions die out rapidly and have no influence on the solutions presented here.

The results obtained with $\omega = 0.001$ can usefully be compared with the steady-state results of Cebeci et al. [30] shown in Fig. 9. We might expect that the small unsteadiness associated with this frequency will lead to results very similar to those of steady state. Inspection of Figs. 7b and 9 shows that although this is correct in general terms, the answers are quantitatively different. As can be seen, the maximum effective angle at which solutions can be obtained is greater in the unsteady case by some 7%. There are differences in the two calculation procedures but it is unlikely that they are responsible for this difference. On the other hand, it is possible that the difference in the negative wall shear values may have been influenced by the use of the FLARE approximation in the steady-state solutions. Nevertheless, the unsteady nature of the flow with $\omega = 0.001$ is clear, in spite of this very low reduced frequency.

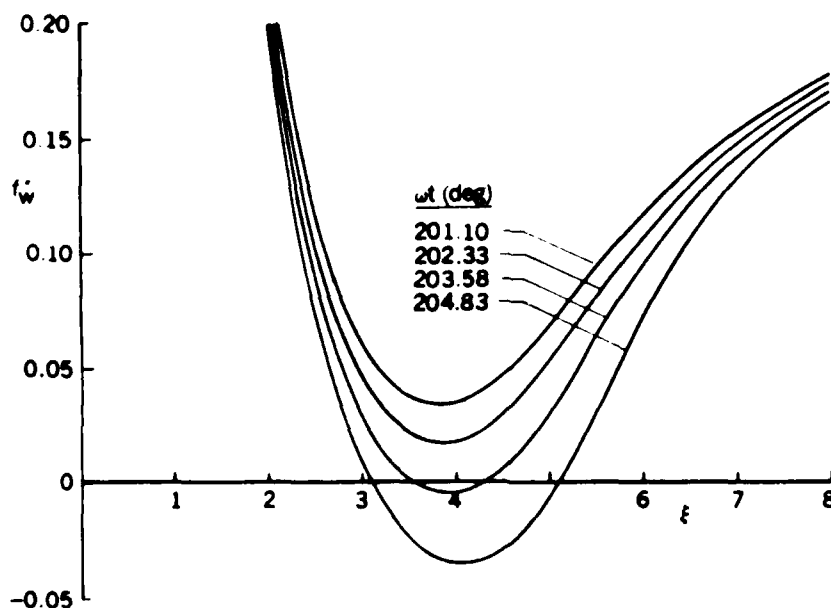


Fig. 9. Effect of interaction on the variation of wall shear parameter f''_w for a steady flow at $R = 10^4$.

4.0 CONJECTURES; SEPARATION BUBBLES AND TRANSITION

An important conclusion from the results of Section 3.3 is that the problem of the singularity, discussed in several papers including that of Cebeci et al. [32], has been overcome by the combined use of an interactive boundary-layer method and a novel numerical scheme with its stability requirements fulfilled. This combination had allowed calculations to be performed but there remains a concern about the physical realism of the long regions of reverse flow predicted in some circumstances. Experiments suggest that leading-edge regions of reverse flow tend to be small with transition to turbulent flow making difficult the existence of long bubbles. This concern is examined by Cebeci [33] in the context of steady flows. It is briefly described in the following paragraphs and the implications of the results for unsteady-flow calculations considered.

As a steady-flow counterpart of the above flows, calculations were performed for the thin airfoil as a function of angle of attack and for the same thickness ratio γ (≈ 0.1) and were reported by Cebeci et al. [30] and Cebeci [33] for Reynolds numbers of 10^6 and 10^5 , respectively. The corresponding distributions of f_w'' are shown on Fig. 10 and have the same form as those presented for the oscillating airfoil. At the highest angle, the separation bubble tends to grow with the number of numerical iterations and suggests that the bubble is unstable.

The large separation bubbles calculated for steady flow seem unrealistic and, at least for the 10^5 Reynolds number where transition is certain to occur downstream of the bubble, there is the possibility that the real flow cannot remain laminar in the region of interest and that this may affect the bubble length. There are, however, no experimental data for airfoils with which to test the possibility and recourse has been made to a different flow for which information of transition is available and which has close similarities to the leading-edge flow.

The experiments of Fage [34] were performed with a series of bumps on a plate and provide information of the location of transition downstream of a region of separated flow caused by the bump and the consequent adverse pressure

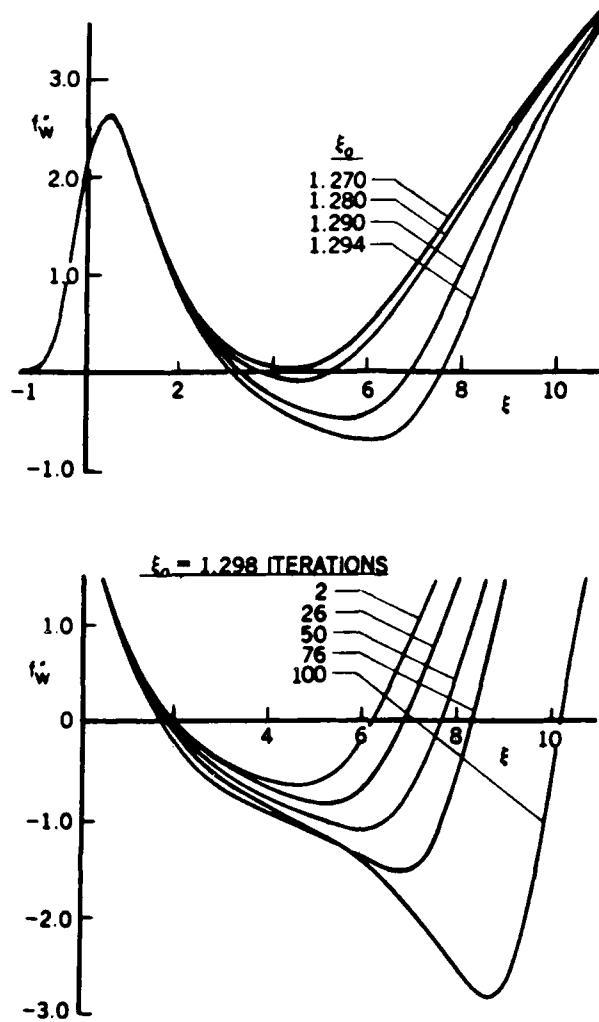


Fig. 10. Separation bubbles and their breakdown - explanation from steady flow (i.e. $\omega = 0$), $R = 10^5$.

gradient. Figure 11 shows the bump and a series of distributions of f_w'' calculated with the interactive procedure: more extensive results have been reported by Cebeci and Egan [35]. The shapes of the f_w'' distributions are similar in form to those of Figs. 8 and 9, downstream from the beginning of the favorable pressure gradient and lend support to the idea that conclusions based on the bump flows can be extrapolated to those on steady and unsteady thin airfoils.

The calculations which led to the results of Fig. 17 provided velocity profiles and those, in turn, were used in the e^n -method of Smith and Gamberoni [36] and of Van Ingen [37] to calculate the location of transition shown on

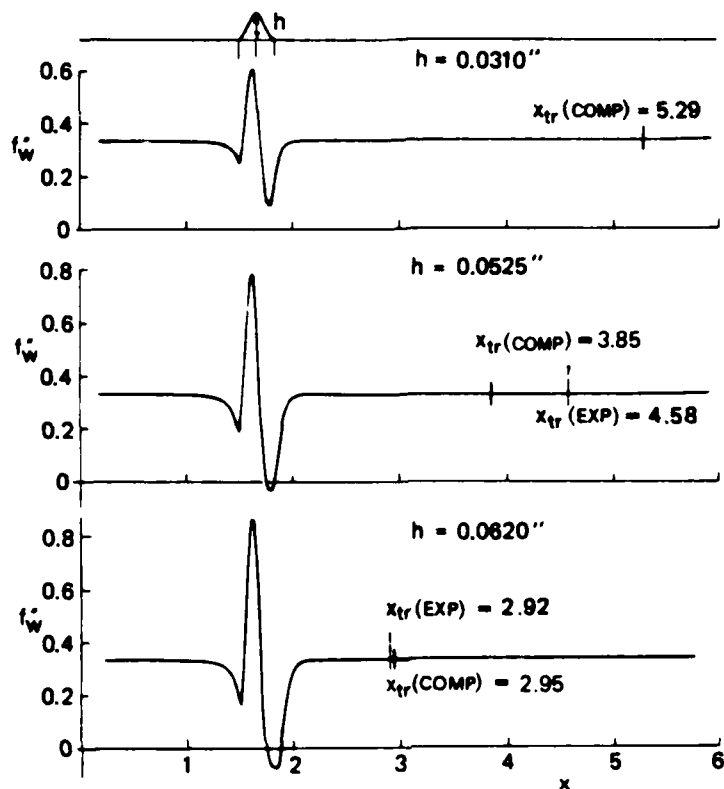


Fig. 11. Accuracy of stability approach to transition. Steady flow over bumps, data of Fage [34].

the figure. This method solves the Orr-Sommerfeld equation for given velocity profiles and computes the amplification rates to determine the location of the onset of transition. As can be seen from Fig. 11, the calculated values of the location of transition agree well with measured values and indicate a clear trend for transition to move upstream with increase in the height of the bump and, therefore, with the strength of the adverse pressure gradient and length of the region of separation. In the case of the largest bump shown, the transition location is inside the bubble and, if the interactive boundary-layer calculations were to be repeated with transition specified at this location, the bubble would be correspondingly reduced in length.

It can be conjectured that the separation bubble would be further shortened as the adverse pressure gradient is increased in strength and transition moves further upstream. This result can be extrapolated to the steady thin-airfoil flows discussed above and their unsteady counterpart. Thus, it seems likely that the long separation bubbles calculated above are unrealistic and in practice would be shortened by transition from laminar to turbulent flow.

5.0 CONCLUDING REMARKS

A series of contributions have been made to the understanding of the flow characteristics of the leading-edge region of an oscillating airfoil. They required the development and use of a calculation method which involves the accurate solution of time-dependent boundary-layer equations and their interaction with solutions to inviscid-flow equations. The need for accurate calculations of regions of reverse flow, including those associated with the moving stagnation point, demanded the use of the characteristic box scheme and the fulfillment of an associated stability requirement. Although those formulated investigations have been made in relation to the model problem of laminar flow in the leading-edge region of a thin airfoil, the calculation method is general and can readily be extended to permit the calculation of the flow around an oscillating airfoil.

Among the specific conclusions which can be drawn are the following:

1. The accuracy of the results obtained from the solution of the boundary-layer equations has been examined with emphasis on regions of flow reversal and separation where the characteristic box scheme is used. Attempts to improve accuracy by ad hoc changes to the finite-difference mesh failed and revealed the need for a procedure which would automatically guarantee accuracy by the selection of an appropriate mesh. This was achieved through a stability criterion, similar to that of Courant, Friedrichs and Lewy [38]. The combination of this requirement and the characteristic box scheme led to accurate solutions and showed that the mesh requirements were extremely severe in the region of large flow reversals.
2. Calculations performed for a range of reduced frequencies from 0 to 0.1 show that increased unsteadiness allows results to be obtained at higher angles of attack before the solutions break down and that, in the case of the highest frequency, there was no breakdown. The calculations with the standard method led to regions of flow reversal which were limited in their extent by the singularity except at the highest frequency. The interactive procedure removed this singularity and resulted in larger regions of flow reversal which involved separation at higher angles of attack.

3. The unsteady nature of the flow at the highest frequency allowed the calculation of large regions of flow reversal and it is expected that yet higher frequencies will lead to even larger regions of flow reversal. This in turn will permit calculations to be performed at larger angles of attack where the occurrence of the singularity will require the use of the interactive procedure. The gains in angles of attack are again likely to be limited by the ability of the laminar flow to sustain separation bubbles and results obtained from the application of linear stability theory suggest that the location of the onset of transition moves upstream with increasing angle of attack and extent of the separation bubble so that it can occur within the bubble. In practice, this would lead to the curtailment of the region of separated flow and the development of a turbulent boundary layer. Support for the accuracy of the calculations of the onset of transition is afforded by comparison of calculated results with measurements in the steady flow over bumps which give rise to distributions of the wall-shear parameter similar to those of airfoil flows.

The research which led to the preceding conclusion is fundamental in nature but has practical implications which should be emphasized. The calculation method has been applied to a model problem and shown to be able to represent unsteady laminar flows with regions of flow reversal and separation. It can equally be applied to calculate the flow over complete airfoils subjected to cyclic or other time-dependent boundary conditions. The additional features to allow these extensions already exist so that, for example, turbulence models have been embodied in a steady-state version of the method and have been shown to represent boundary-layer and wake flows with accuracy close to that of the test measurements; steady-state calculations of transitional flows, including those with flow separation, have been examined and shown to be calculable; and a foundation has been laid for the calculation of flows around components of aircraft. With this catalogue of achievements, it is recommended that work be carried out to develop the method further and to apply it to problems including those associated with helicopter blades and the maneuverability of aircraft such as the X-31 so that the merits of different designs can be assessed. It is particularly appropriate that it be used to study flows associated with angles of attack close to those of static and dynamic stall.

6.0 REFERENCES

1. McCroskey, W.J., McAlister, K.W., and Carr, L.W., "Dynamic Stall Experiments on Oscillating Airfoils," AIAA Journal, Vol. 14, Jan. 1976, pp. 57-63.
2. Carr, L.W., McAlister, K.W. and McCroskey, W.J., "Analysis of the Development of Dynamic Stall Based on Oscillating Airfoil Experiments," NASA TN D-8382, 1977.
3. Dadone, L.U., "Two-Dimensional Wind Tunnel Test of an Oscillating Rotor Airfoil," NASA CR-2914, Dec. 1977.
4. Francis, M.S., Keese, J.E. and Retelle, J.P., Jr., "An Investigation of Airfoil Dynamic Stall with Large Amplitude Motions," FJSRL-TR-83-0010, F.J. Seiler Research Labs, Air Force Academy, Colorado Springs, 1983.
5. Daley, D.C. and Jumper, E.J., "Experimental Investigation of Dynamic Stall for a Pitching Airfoil," Journal of Aircraft, Vol. 21, Oct. 1984, pp. 831-832.
6. Francis, M.S. and Keese, J.E., "Airfoil Dynamic Stall Performance with Large Amplitude Motions," AIAA Journal, Vol. 23, Nov. 1985, pp. 1653-1659.
7. Lorber, P.F. and Covert, E.E., "Unsteady Airfoil Boundary Layers - Experiment and Computation," in Numerical and Physical Aspects of Aerodynamic Flows III (T. Cebeci ed.), Springer-Verlag, N.Y., 1986, pp. 235-251.
8. Lorber, P.F. and Carta, F.O., "Unsteady Stall Penetration Experiments at High Reynolds Number," United Technologies Research Center Report R87-956939-3, Apr. 1987 (to be released as a technical report by the U.S. Air Force Office of Scientific Research).
9. Shamroth, S.J., "A Turbulent-Flow Navier-Stokes Analysis for an Airfoil Oscillating in Pitch," in Unsteady Turbulent Shear Flows (R. Michel, J. Cousteix and R. Houdeville, eds.), Springer-Verlag, 1981, pp. 185-196.
10. Cebeci, T. and Carr L.W., "Prediction of Boundary-Layer Characteristics of an Oscillating Airfoil," in Unsteady Turbulent Shear Flows (R. Michel, J. Cousteix and R. Houdeville, eds.), Springer-Verlag, 1981, pp. 145-158.
11. Cebeci, T. and Carr, L.W., "Calculation of Boundary Layers Near the Stagnation Point of an Oscillating Airfoil," NASA TM 84305, 1983.
12. Cebeci, T. and Carr, L.W., "An Interactive Boundary-Layer Method for Oscillating Airfoils: Status and Prognosis," NASA Report in preparation.
13. Lang, J.D., "Unsteady Aerodynamics and Dynamic Aircraft Maneuverability," AGARD CP-386, Unsteady Aerodynamics - Fundamentals and Application to Aircraft Dynamics, Nov. 1985.
14. Heibst, W.B., "Supermaneuverability," Proceedings of the AFOSR-FJSRL-University of Colorado Workshop on Unsteady Separated Flows, U.S. Air Force Academy, Colorado Springs, Aug. 1983.

15. Geissler, W., "Unsteady Boundary-Layer Separation on Airfoils Performing Large Amplitude Oscillations - Dynamic Stall," AGARD Symposium on Unsteady Aerodynamics, Fundamentals and Applications to Aircraft Dynamics, Gottingen, Germany, 1985.
16. Maskew, B. and Dvorak, F.A., "Prediction of Dynamic Separation Characteristics Using a Time-Stepping Viscid/Inviscid Approach," in Numerical and Physical Aspects of Aerodynamic Flows III (T. Cebeci, ed.) Springer-Verlag, N.Y., 1986, pp. 380-396.
17. Teng, N.G., "The Development of a Computer Code (U2DIIF) for the Numerical Solution of Unsteady, Inviscid and Incompressible Flow Over an Airfoil," M.S. Thesis, Department of Aeronautics, Naval Postgraduate School, Monterey, CA, 1987.
18. Crank, J. and Nicolson, P., "A Practical Method of Numerical Evaluation of Solutions of Partial-Differential Equations of the Heat-Conduction Type," Proceedings of Cambridge Philosophical Society, Vol. 43, 1947, p. 50.
19. Keller, H.B., "Accurate Difference Methods for Two-Point Boundary-Value Problems," SIAM Journal of Numerical Analysis, Vol. 11, 1974, pp. 305-320.
20. Keller, H.B., "Numerical Methods in Boundary-Layer Theory," Annual Review of Fluid Mechanics, Vol. 10, 1978, pp. 417-433.
21. Cebeci, T., "Unsteady Boundary Layers with an Intelligent Numerical Scheme," Journal of Fluid Mechanics, Vol. 163, 1986, p. 129.
22. Krause, E., Hirschel, E.H. and Bothman, Th., "Die Numerische Integration der Bewegungsgleichungen Dreidimensionaler Laminarer Kompressibler Grenzschichten," Band 3, Fachtagung Aerodynamic, Berlin; D6LR-Fachlinchreihe, 1968.
23. Cebeci, T., Khattab, A.A. and Schimke, S.M., "Separation and Reattachment Near the Leading Edge of a Thin Oscillating Airfoil," to be published in Journal of Fluid Mechanics, 1988.
24. Veldman, A.E.P., "New Quasi-Simultaneous Method to Calculate Interacting Boundary Layers," AIAA Journal, Vol. 19, 1981, p. 769.
25. LeBalleur, J.C., "Couplage visqueux-nonvisquex: Methode Numerique et Applications Aux Ecoulements Bidimensionnels Transoniques et Supersoniques," Le Recherche Aerospatiale No. 1978-2, 1978, p. 65.
26. Carter, J.E., "A New Boundary-Layer Inviscid Interaction Technique for Separated Flow," AIAA Paper 79-1450, 1979.
27. Cebeci, T., Clark, R.W., Chang, K.C., Halsey, N.D. and Lee, K., "Airfoils with Separation and the Resulting Wakes," Journal of Fluid Mechanics, Vol. 163, 1986, p. 323.
28. Cebeci, T., Sedlock, D., Chang, K.C. and Clark, R.W., "Applications of Two- and Three-Dimensional Interactive Boundary-Layer Theory to Finite Wings with Flow Separation," AIAA Paper No. 87-0590, 1987.

29. Cebeci, T., Kaups, K. and Khattab, A.A., "Separation and Reattachment Near the Leading Edge of a Thin Wing," IUTAM Proceedings, London, Aug. 1986.
30. Cebeci, T., Stewartson, K. and Williams, P.G., "Separation and Reattachment Near the Leading Edge of a Thin Airfoil at Incidence," AGARD CP-291, Paper 20, 1981.
31. Cebeci, T., Simoneau, R.J. and Platzer, M.F., "A General Method for Unsteady Heat Transfer on Turbine Blades," NASA CR in preparation.
32. Cebeci, T., Khattab, A.A. and Schimke, S.M., "Can the Singularity be Removed in Time-Dependent Flows?," in Workshop on Unsteady Separated Flow (M.S. Francis and M.W. Luttges, eds.), Colorado Springs, 1984.
33. Cebeci, T., "Instability of Laminar Separation Bubbles: Causes and Effects," paper in review.
34. Fage, A., "The Smallest Size of Spanwise Surface Corrugation which Affects Boundary-Layer Transition on an Airfoil," R&M No. 2120, Brit. A.R.C., 1943.
35. Cebeci, T. and Egan, D., "The Effect of Wave-Like Roughness on Transition," paper in preparation.
36. Smith, A.M.O. and Gamberoni, N., "Transition, Pressure Gradient and Stability Theory," Proc. IX Intl. Congress Applied Mechanics, Brussels, 1956.
37. Van Ingen, J.L., "A Suggested Semi-Empirical Method for the Calculation of the Boundary-Layer Transition Region," Report No. VTH71, VTH74, Delft, Holland, 1956.
38. Isaacson, E. and Keller, H.B., Analysis of Numerical Methods, John Wiley, N.Y., 1966.

REPORT DOCUMENTATION PAGE				
1a. REPORT SECURITY CLASSIFICATION Unclassified		1d. RESTRICTIVE MARKINGS		
2a. SECURITY CLASSIFICATION AUTHORITY		3. DISTRIBUTION/AVAILABILITY OF REPORT Approved for public release; distribution unlimited		
2b. DECLASSIFICATION/DOWNGRADING SCHEDULE				
4. PERFORMING ORGANIZATION REPORT NUMBER(S) MDC K0535		5. MONITORING ORGANIZATION REPORT NUMBER(S) AFOSR-TR. 87-1779		
6a. NAME OF PERFORMING ORGANIZATION Douglas Aircraft Company		6b. OFFICE SYMBOL (if applicable)	7a. NAME OF MONITORING ORGANIZATION Air Force Office of Scientific Research	
6c. ADDRESS (City, State and ZIP Code) 3855 Lakewood Blvd. Long Beach, CA 90846		7b. ADDRESS (City, State and ZIP Code) Bolling AFB Washington, DC 20332		
8a. NAME OF FUNDING/SPONSORING ORGANIZATION Air Force Office of Scientific Research		8b. OFFICE SYMBOL (if applicable) AFOSR/NA	9. PROCUREMENT INSTRUMENT IDENTIFICATION NUMBER F49620-87-C-0004	
8c. ADDRESS (City, State and ZIP Code) Building 410 Bolling AFB Washington, DC 20332		10. SOURCE OF FUNDING NOS.		
		PROGRAM ELEMENT NO. 61102F	PROJECT NO. 2307	TASK NO. A3
11. TITLE (Include Security Classification) OSCILLATING AIRFOILS - ACHIEVEMENTS AND CONJECTURES (U)				
12. PERSONAL AUTHOR(S) Tuncer Cebeci				
13a. TYPE OF REPORT Technical FINAL		13b. TIME COVERED FROM 10/86 TO 9/87	14. DATE OF REPORT (Yr., Mo., Day) 87 Sept	15. PAGE COUNT 26
16. SUPPLEMENTARY NOTATION				
17. COSATI CODES			18. SUBJECT TERMS (Continue on reverse if necessary and identify by block number) Unsteady Flows Separation, Reattachment Oscillating Airfoil Transition, Turbulence Singularity Interactive Boundary-Layer Theory	
FIELD	GROUP	SUB. GR.		
01	01			
20	04			
19. ABSTRACT (Continue on reverse if necessary and identify by block number) Recent developments and applications of an interactive boundary-layer procedure for unsteady flows are reviewed. The emphasis is on a model problem corresponding to an oscillating thin airfoil in laminar flows and results are reported for different amplitudes and frequencies of oscillation. The use of the characteristic box scheme, with its stability criterion, are shown to allow the accurate calculation of reverse flows and the interaction procedure removes the singularity to allow calculation through regions of separated flow. Although the current focus of the interactive boundary-layer procedure has been on the leading-edge region, it has general applicability and, together with models for transition and turbulent flows, it can provide the basis for a method to deal with oscillating airfoils and wings and the rapid movement of fixed-wing arrangements at angles of attack up to and beyond those of dynamic stall.				
20. DISTRIBUTION/AVAILABILITY OF ABSTRACT UNCLASSIFIED/UNLIMITED <input checked="" type="checkbox"/> SAME AS RPT. <input type="checkbox"/> DTIC USERS <input type="checkbox"/>			21. ABSTRACT SECURITY CLASSIFICATION Unclassified	
22a. NAME OF RESPONSIBLE INDIVIDUAL Dr. James D. Wilson		22b. TELEPHONE NUMBER (Include Area Code) (202) 767-4935	22c. OFFICE SYMBOL AFOSR/NA	

Unclassified

SECURITY CLASSIFICATION OF THIS PAGE

Calculations at high angles of attack indicate that the behavior of the unsteady separated leading-edge flow has similarities to steady flows downstream of surface corrugations. The use of linear stability theory in the latter case shows that the location of the onset of transition moves upstream with severity of corrugation and can move inside the separation bubble. In practice this means that the bubbles will be shortened and analogy with unsteady flows suggests that transition may play an important role and preclude the existence of the long separation bubbles determined by the laminar-flow calculations.

Unclassified

SECURITY CLASSIFICATION OF THIS PAGE

END
DATE
FILMED

4-88

DTIC